[CANCER RESEARCH 63, 5178–5187, September 1, 2003]

Advances in Brief

Alternative Splicing of the Human Proto-oncogene c-H-*ras* Renders a New Ras Family Protein That Trafficks to Cytoplasm and Nucleus[1,2]

Sònia Guil, Núria de La Iglesia, Juan Fernández-Larrea, Daniel Cifuentes, Juan C. Ferrer, Joan J. Guinovart, and Montse Bach-Elias[3]

Centre d'Investigació Cardiovascular-Consejo Superior de Investigaciones Científicas (CIC-CSIC), Barcelona [S. G., M. B-E.], Fontlab 2000 s.l., St. Eulalia de Ronçana [J. F-L.], and Departament de Bioquímica i Biologia Molecular, Universitat de Barcelona, 08034 Barcelona [N. d. L. I., D. C., J. C. F., J. J. G.], Spain

Abstract

We characterized a novel protein of the Ras family, p19 (H-RasIDX). The c-H-*ras* proto-oncogene undergoes alternative splicing of the exon termed IDX. We show that the alternative p19 mRNA is stable and as abundant as p21 (p21 H-Ras4A) mRNA in all of the human tissues and cell lines tested. IDX is spliced into stable mRNA in different mammalian species, which present a high degree of nucleotide conservation. Both the endogenous and the transiently expressed p19 protein are detected in COS-1 and HeLa cells and show nuclear diffuse and speckled patterns as well as cytoplasmic localization. In yeast two-hybrid assays, p19 did not interact with two known p21 effectors, Raf1 and Rin1, but was shown to interact with RACK1, a scaffolding protein that promotes multiprotein complexes in different signaling pathways. This observation suggests that p19 and p21 play differential and complementary roles in the cell.

Introduction

Mammalian cells contain three functional c-*ras* genes, known as c-H-*ras*, c-K-*ras*, and c-N-*ras*, the study of which has generated essential data about normal and tumorigenic signal transduction events (reviewed in Refs. 1–3). Ras proteins are GTPases that bind to GTP and GDP nucleotides. The switch between their inactive (GDP-bound) and active (GTP-bound) forms, together with their ability to bind to target proteins, provides the mechanism for the downstream transmission of the cellular signals. These signals are transduced by a cascade of biochemical modifications of protein factors that regulate several pathways affecting cell cycle progression. Depending on the nature of the stimulus, this cascade can finally induce proliferation, differentiation, growth arrest or apoptosis of normal cells (1–3).

In 1989, Cohen *et al.* (4) reported that H-Ras pre-mRNA has an alternative splicing of the last encoding exon. The c-H-*ras* gene could then render two mRNAs, one with a stop codon on exon 4A (E4A) and a second message with a stop codon on the exon termed IDX (see Fig. 1). Message E0-E1-E2-E3-E4A-E4B is translated into the p21 protein (H-Ras4A), and because IDX contains an in-frame stop codon, the alternative message E0-E1-E2-E3-IDX-E4A-E4B might yield a hypothetical p19 protein (H-RasIDX). These authors suggested that p19 mRNA should be unstable because it contains a premature stop codon on the IDX exon, which could be recognized as a nonsense codon and therefore be degraded by a nonsense-mediated decay mechanism (4). They also reported that one of the products of this alternative splicing, p19 mRNA, lacked transforming potential and showed that the transforming activity of the H-*ras* gene is inversely proportional to the efficiency of the alternative splicing of the H-Ras pre-mRNA toward p19 mRNA (4). Later, Huang and Cohen (5) suggested that a putative p19 protein could act as a negative regulator of the p21 protein. Recently, Guil *et al.* (6) demonstrated that hnRNP A1, SR proteins, and p68 RNA helicase regulate this alternative splicing.

Materials and Methods

Cell Culture, RNA Preparation, and Total Protein Extracts

HeLa, Rat-1, COS-1, and NIH/3T3 cells were grown as described previously (7). Total RNA was obtained as described elsewhere (8). Nuclear protein extracts were prepared as described previously (9). Total SDS extracts were obtained by sonication of cell pellets in SDS-PAGE protein sample buffer. The sources of total RNA from the different species were as follows: COS-1, monkey cultured cells; NIH/3T3, mouse cultured cells; Rat-1, rat cultured cells; and liver from pig, rabbit, and cow. Purification of GST[4] recombinant proteins were performed according the instructions in the GSTrap manual (Pharmacia).

Antibodies, Antibody Purification, and Western Blots

Antibodies against p19 protein were raised in rabbits, using the peptide GSRSGSSSSSGTLWD, which includes 15 of the 20 amino acids of the human IDX sequence, plus a Cys at the COOH-terminal end to allow coupling to keyhole limpet hemocyanin, as detailed elsewhere (10). Preimmune sera from the same rabbits were obtained before immunization. The sera were tested by Western blot analyses of total bacterial extracts from cells (*Escherichia coli*, strain BL21) expressing either the recombinant GST-p19 or GST-p21 proteins as antigen sources. The bacterial extracts were obtained as detailed elsewhere (11). One immunoreactive serum was selected and named SP1.[5] Specific antibodies reacting with the peptide were purified from the crude SP1 serum by use of a peptide immunoaffinity column as described previously (10). The specificity of the purified antibody was analyzed again by a peptide ELISA and Western blot analysis (10). Rabbit anti-p21 antibodies (C-20), which recognize the COOH terminus of p21, were purchased from Santa Cruz Biotechnology Inc. C-20 antibody did not cross-react with GST-p19 protein or endogenous p19 protein, as assayed by Western blots. Mouse monoclonal anti-SC-35 antibodies were purchased from BD PharMingen.

Plasmid Constructions

All plasmid inserts were obtained by PCR using *Pfu* DNA polymerase (Stratagene). All constructs were verified by DNA sequencing.

Received 3/13/03; revised 6/23/03; accepted 6/30/03.

The costs of publication of this article were defrayed in part by the payment of page charges. This article must therefore be hereby marked *advertisement* in accordance with 18 U.S.C. Section 1734 solely to indicate this fact.

[1] This work was supported by Fundación Ramón Areces, but was started with a grant from the Asociación Española contra el Cáncer and La Marató de TV3. S. G. was a recipient of a BEFI fellowship.

[2] Supplementary data for this article are available at *Cancer Research* Online (http://cancerres.aacrjournals.org).

[3] To whom requests for reprints should be addressed, at IIBB-CSIC. C/Jorge Girona Salgado 18-26, 08034 Barcelona, Spain. Phone: 34-93-4006134; Fax: 34-93-2045904; E-mail: mbebmc@cid.csic.es.

[4] The abbreviations used are: GST, glutathione *S*-transferase; GFP, green fluorescent protein; IF, immunofluorescence; TRITC, tetramethylrhodamine isothiocyanate; RT-PCR, reverse transcription-PCR; MTE, multiple tissue expression; nt, nucleotide; EST, expressed sequence tag; UsnRNP, U small nuclear ribonucleoprotein; IGC, interchromatin granule cluster; PKC, protein kinase C.

[5] SP1 serum will be provided by Fontlab 200 s.l. (Fontlab2000@telelin.es).

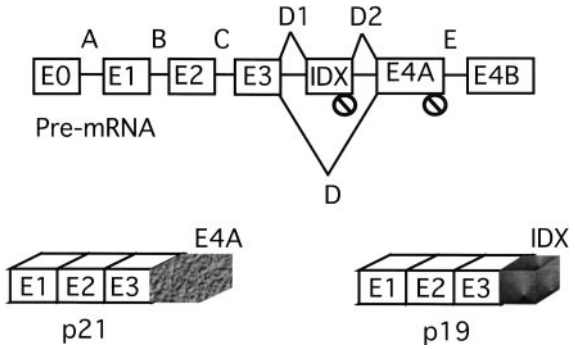

Fig. 1. Alternative splicing of H-*ras* gene. The position of the in-frame stop codons (⦸) are indicated on the pre-mRNA.

Human and Rat Riboprobes for RNase Protection Assays

A fragment containing human IDX and E4A was obtained from HeLa cDNA with primers IDXfor and D2/848 and cloned in pGEM-T-easy (Promega) with the antisense strand under the control of the T7 promoter. The plasmid was linearized with *Sma*I and transcribed with T7 RNA polymerase in the presence of [α-^{32}P]CTP.

Anti-E4A Riboprobe for Exonic Northern Blot

The fragment of the human E4A was amplified from HeLa cDNA by PCR with primers E4Afor and D2/848 and cloned in the *Ecl*136I site of pBluescript SK(−). The plasmid was linearized with *Eco*RV before transcription of the antisense strand by T3 RNA polymerase.

Anti-IDX Riboprobe for Exonic Northern Blot

Anti-IDX riboprobe was obtained in a manner analogous to that for the anti-E4A riboprobe but with use of the IDXfor and IDXrev oligodeoxynucleotides. The antisense strand of IDX was transcribed with T3 RNA polymerase after the plasmid was linearized with *Not*I.

GST-p19 Expression Vector

A fragment coding for p19 was amplified from HeLa cDNA by PCR using the primers E1for and IDX-GSTrev. The PCR product was digested with *Bam*HI and *Eco*RI and cloned into the same sites in pGEX-4T-3 (Pharmacia).

GST-p21 Expression Vector

GST-p21 expression vector was obtained similar to that for GST-p19 but with use of p21-GSTrev primer instead of IDX-GSTrev.

GFP-p19 and GFP-p21 Expression Vectors

The PCR fragments encoding p19 and p21 were obtained as described above, but with use of the primers GFP-p19dir and GFP-p19rev or GFP-p21rev. After digestion with *Eco*RI and *Bam*HI, these fragments were ligated into pEGFP-C1 (Clontech), cut with the same enzymes. To construct the plasmid (ΔGFP)-p19, a PCR fragment of the p19 mRNA was obtained with primers p19Kozakfor and GFP-p19rev. This fragment was identical to the one used for the GFP-p19 plasmid, but it included at its 5′ end a Kozak consensus sequence that enhanced translation of the protein. After the PCR fragment and the pEGFP-N3 vector (Clontech) were digested with *Eco*RI and *Bam*HI and ligated, the resulting plasmid was recut with *Bam*HI and *Not*I (which deletes most of the GFP coding region), blunt-ended, and religated.

Mutants Gly12Val (mut12) and Ser17Arg (N17)

The Gly12Val (mut12) and Ser17Arg (N17) mutants were obtained from (ΔGFP)-p19 by PCR using the Quick-site directed mutagenesis kit (Stratagene) with primers Gly12Valdir/Gly12Valrev and Ser17Argdir/Ser17Argrev.

Yeast Two-Hybrid Plasmids

Plasmids containing full-length cDNA for human Raf1 (GenBank accession no. NM_002880) or Rin1 (GenBank accession no. NM_004292) were a generous gift from Dr. Michael A. White (12). Full-length cDNAs encoding human p19, p21, Raf1, or Rin1 were obtained by PCR amplification using the corresponding templates and appropriate oligonucleotides as primers and were fused in frame with the GAL4 activation domain in the pGADT7vector (Clontech) or with the GAL4 DNA-binding domain in the pGBKT7vector (Clontech). In all cases, the cloning site was *Eco*RI–*Bam*HI in the polylinker of both plasmids. pGBKT7-IDX was obtained from pGBKT7-p19 by PCR of the region encompassing the IDX sequence with suitable primers. pACT2-RACK1 was obtained from the human cDNA library during the screening by the yeast two-hybrid assay (Clontech).

RNase T1 Protection Assay

RNase T1 protection assay shown in Fig. 2*A* was performed with total HeLa RNA. We mixed 2 μg of total RNA with 10^5 cpm of riboprobe in hybridization buffer [40 mM PIPES (pH 6.4), 1 mM EDTA, 0.4 M NaCl, and 80% formamide] in a total volume of 30 μl. After heating at 85°C for 10 min, the mixture was incubated overnight at 55°C. Unhybridized probe was digested for 15 min at 30°C with 300 μl of RNase buffer [300 mM NaCl, 10 mM Tris-HCl (pH 7.4), 5 mM EDTA] containing 0.5 units/μl RNase T1. After protein digestion and ethanol precipitation, the protected fragments were resolved in a 6% urea/polyacrylamide gel. pBR-322 cut with *Hpa*II and 5′-end-labeled with [γ-^{32}P]ATP was used as molecular weight marker.

GTP-binding Assays

GTP-binding assays were performed according the protocol described by Pieper *et al.* (13).

IF and Confocal Fluorescence Microscopy

GFP Images. COS-1 and HeLa cells were seeded onto coverslips the day before transfection. Transfection was performed at 60–70% confluence with SuperFect Transfection Reagent (Qiagen) using 2.5 μg of GFP-p19 or GFP-p21 expression plasmids per 35-mm dish. After overnight incubation, cells were fixed with 4% paraformaldehyde and washed twice in PBS, and the coverslips were mounted on glass slides as described previously (7).

Indirect IF Images. COS-1 and HeLa cells were transfected with the plasmids described in the legend for Fig. 4 as for the GFP images. After paraformaldehyde fixation, cells were treated with $NaBH_4$ (1 mg/ml), permeabilized with 0.2% (v/v) Triton X-100, and blocked with 3% BSA-PBS. p19 expression was visualized by use of either the crude SP1 serum or immunoaffinity-purified SP1 antibodies (dilution 1:10 or 1:50 for detection of endogenous or overexpressed protein, respectively) as described previously (7). IF detection of endogenous SC-35 was performed by incubation of the cells with the anti-SC-35 antibody (1:50 dilution). Double staining of the cells with SP1 immunoaffinity-purified and SC-35 antibodies was performed on cells transiently transfected with the (ΔGFP)-p19 plasmid in the same way. Primary antibodies were detected either by TRITC-labeled anti-rabbit or FITC-labeled anti-mouse antibodies. Fluorescence images were obtained with a Leica TCS 4D (Leica Lasertechnik) confocal scanning laser microscope adapted to an inverted Leitz DMIRBE microscope and a ×63/1.4 oil Plan-Apo objective. The light source was an argon/krypton laser (75 mW). Green fluorescence from GFP recombinants or FITC-conjugated secondary antibodies and red fluorescence from TRITC-conjugated secondary antibodies were excited at 488 and 568 nm, respectively. Optical sections of 0.5 μm were obtained, and colocalization analysis was performed with Metamorph Imaging System software (version 3.5; Universal Imaging Corporation).

RT-PCR and Oligodeoxynucleotides

RT-PCRs were performed as indicated previously (14). All PCR bands obtained were sequenced. New E3-IDX-E4A sequences were obtained by

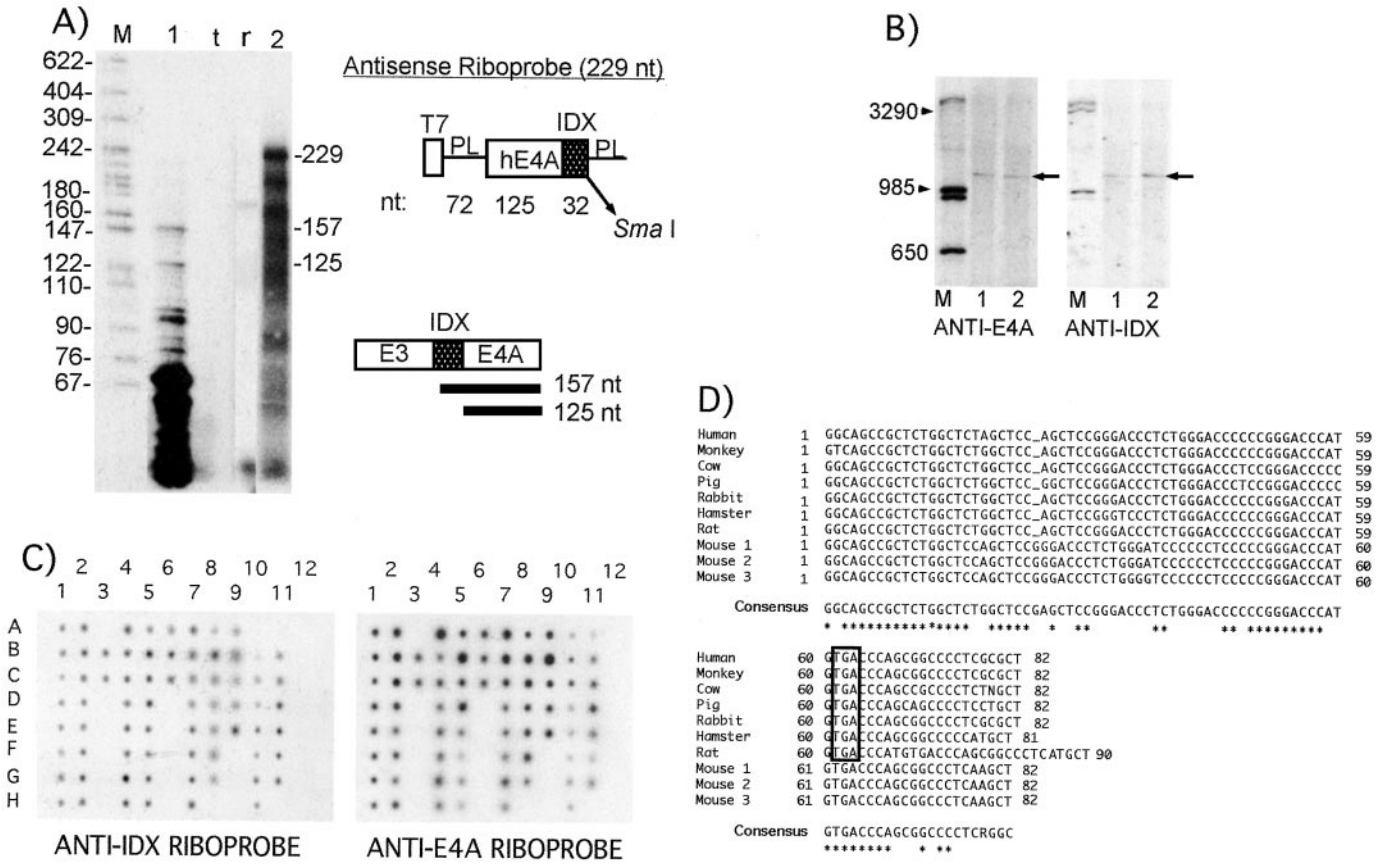

Fig. 2. p19 mRNA is as abundant as p21 in human cells and is stably expressed. *A*, relative abundance of human p19 mRNA in HeLa cells. One specific exonic antisense radiolabeled riboprobe was generated to quantify the relative abundance of p19 and p21 mRNAs. *Lane 1* contains total RNA extracted from HeLa cells bound to the riboprobe and digested with RNase T1. *Lane 2* is a control of the riboprobe mixed with RNA and not subjected to RNase T1 digestion. *Lane t* contains a mixture of total yeast tRNA and the riboprobe, which was also digested with RNase T1. *Lane r* contains total rat RNA from Rat-1 cells and the human riboprobe digested with RNase T1. *Lane M* contains the molecular weight marker. The expected size of the protected fragments is indicated to the *right* of the gels. *B*, detection of p19 mRNA by exonic Northern assays in total RNA from HeLa cells. Two specific antisense radiolabeled riboprobes were generated: one directed to E4A (anti-E4A riboprobe) and the other directed to IDX (anti-IDX riboprobe) of the human c-H-*ras* gene. Thus the anti-E4A probe recognizes both human p19 and p21 mRNAs, and the anti-IDX radioprobe recognizes only p19 mRNA. The blot with the anti-E4A riboprobe (*left*) was assayed first; the membrane was then stripped out and hybridized with the anti-IDX riboprobe (*right*). Identical results were obtained when the order of hybridizations was reversed. *Lanes M*, specific DNA molecular markers detailed in the "Materials and Methods:" the 3290-nt band is a *Pst*I–*Bam*HI fragment of the c-H-*ras* gene that includes the IDX sequence (and not the E4A sequence); the 985-nt band is a *Kpn*I–*Bam*HI fragment that contains both the IDX and the E4A sequences, and the 650-nt band is a *Pst*I–*Bam*HI fragment that includes the E4A sequence (and not the IDX sequence). *Lanes 1* and *2* contained 20 μg of total HeLa RNA from two independent RNA preparations. Superposition of both autoradiographs (*left* and *right*) showed that the detected bands, marked with *arrows*, migrated the same distance. The different band intensities do not reflect the mRNA quantities because probes with different specific activities were used in these assays. *C*, exonic Northern dot-blot assay on MTE array. The Northern dot blot was incubated with anti-IDX riboprobe (*left*) and the anti-E4A riboprobe (*right*). Tissues and quantification are shown in Supplemental Table 1. *D*, conservation of IDX sequences across species. The aligned sequences of several IDX nucleotide sequences are shown. These sequences were obtained either from GenBank or by sequencing the corresponding cDNAs obtained by RT-PCR (PCR performed with *Pfu*) of total RNA from several species and using specific primers directed to E3 and E4A. The in-frame stop codon is *boxed* (note that mouse does not have an in-frame stop codon in the IDX exon; see "Results"). Sequences were aligned with the MacMolly Tetra program, version 3.8 (Soft Gene GmbH) with the specification that the first three IDX nucleotides constitute the first IDX translated codon. The nucleotides that are 100% conserved are indicated with $*$ in the consensus sequence. The GenBank accession numbers are as follows, with new sequences obtained in this work indicated by a superscripted "*a*": human (*Homo sapiens*; BC006499.1); monkey[a] (COS-1 cultured cells; *Cercopithecus aethiops*, new GenBank accession no. AJ437019); cow[a] (*Bos taurus*, new GenBank accession no. AJ437020); pig[a] (*Sus scrofa*; new GenBank accession no. AJ437021); rabbit[a] (*Oryctolagus cuniculus*; new GenBank accession no. AJ437022); hamster (*Mesocricetus auratus*; GenBank accession no. M84166.1); rat (Rat-1 cultured cells; *Rattus norvegicus*; see Ref. 4); mouse 1 (strain 129/SvJ; *Mus musculus*; GenBank accession no. AF081118); mouse 2 (*Mus musculus*; GenBank accession no. BI731283); and mouse 3[a] (NIH/3T3 cultured cells, *Mus musculus*; new GenBank accession no. AJ437024). As indicated in the "Results," different mouse and rat IDX sequences deposited in GenBank presented nucleotide discrepancies. They were therefore resequenced in this work.

RT-PCR of total RNA using oligo-dT, Superscript Reverse Transcriptase (Life Technologies) and *Pfu* DNA polymerase in three independent experiments.

Oligodeoxynucleotides (all given as 5′–3′) were as follows:

E3for: GGA GCA GAT CAA ACG GGT GA;

E4Arev: CTG CCG GAT CTC ACG CAC CA;

ratE4rev: CTA GTG TCA GGA CAG CAC AC;

IDXfor: GGC AGC CGC TCT GGC TCT AG;

D2/848: AGT CCC CCT CAC CTG CGT CA;

IDXrev: CGC GAG GGG CCG CTG GGT CA;

E1for: CGA TGG GAT CCT ATG ACG GAA TAT AAG CTG GTG GTG;

IDX-GSTrev: CTG TCG AAT TCT CAC ATG GGT CCC GGG GGG TCC CA;

p21-GSTrev: CTG TCG AAT TCT CAG GAG AGC ACA CAC TTG CAG CT;

GFP-p19dir: CTG TCG AAT TCT ATG ACG GAA TAT AAG CTG GTG GTG;

GFP-p19rev: CGA TGG GAT CCT CAC ATG GGT CCC GGG GGG TCC CA;

GFP-p21rev: CGA TGG GAT CCT CAG GAG AGC ACA CAC TTG CAG CT;

p19-Kozakfor: CTG TCG AAT TCC GCC ACC ATG ACG GAA TAT AAG CTG GTG;

Gly121Valdir: GTG GTG GGC GCC GTC GGT GTG GGC AAG;

Gly12Valrev: CTT GCC CAC ACC GAC GGC GCC CAC CAC;

Ser17Argdir: GGT GTG GGC AAG AAT GCG CTG ACC ATC;

Ser17Argrev: GAT GGT CAG CGC ATT CTT GCC CAC ACC;

5′HRasp21/p19dir: CAT ATG GAA TTC ATG ACG GAA TAT AAG CTG GTG G;

3′HRasp21 humrev: AAG CTT GGA TCC TCA GGA GAG CAC ACA C;

3′HRasp19 humrev: AAG CTT GGA TCC TCA CAT GGG TCC CG;

5′Raf1 humdir: CAT ATG GAA TTC ATG GAG CAC ATA CAG GG;

3′Raf1 humrev: TCT CGA GGA TCC CTA GAA GAC AGG CAG C.

Yeast Two-Hybrid Assays

Pairwise protein-protein interactions were assayed in the yeast strain AH109 (Clontech) after cotransformation with bait-and-prey constructs. Primary cotransformants were selected on double drop-out media (−Leu/−Trp). To test interactions, we separately grew five independent Leu+/Trp+ colonies arising from each cotransformation experiment to saturation in −Leu/−Trp liquid medium, brought together, and 5 μl of this mixed culture were dropped on solid quadruple drop out medium (−Leu/−Trp/−His/−Ade). Colony growth was scored after 5 days of incubation at 30°C.

Exonic Northern Blot on Total HeLa RNA and Exonic Northern Blot on a MTE Array

Exonic Northern blots were performed as described previously (15). We electrophoresed 20 μg of total RNA from HeLa cells in 5% acrylamide/urea gels and blotted the gels on Hybond-N nylon membranes (Amersham). Anti-E4A and anti-IDX riboprobes (antisense sequences) were homogeneously labeled by transcription with [α-^{32}P]CTP. IDX riboprobe showed no homology to other sequences in the human genome data bank; E4A riboprobe was designed to bind the hypervariable region of c-H-*ras* and does not cross-react with N- or K-*ras* sequences. To use the probes in the same blot, we first bound one probe to the RNA blot and autoradiographed. The bound probe was stripped out by washing as described previously (15), and the remaining radioactivity was checked by autoradiography before assaying with the second probe. Identical results were obtained regardless of whether the E4A riboprobe or the IDX riboprobe was used first. Specific Northern markers for this assay were prepared: the restriction fragment *Nco*I–*Bam*HI from the c-H-*ras* gene was cloned into the *Sma*I site of pBluescript SK(−) and cut with different restriction enzymes; a mixture of all digestions was loaded on the same gel and blotted together with the RNA samples. The 3290-nt band was a *Pst*I–*Bam*HI fragment and contained the IDX sequence but not the E4A sequence; the 985-nt band was a *Kpn*I–*Bam*HI fragment and contained both IDX and E4A sequences, whereas the 650-nt band was also a *Pst*I–*Bam*HI fragment containing the E4A sequence but not the IDX sequence. The Northern dot blot membrane (MTE) was purchased from Clontech and was assayed with the riboprobes described above. This nylon membrane contained normalized loading of polyA$^+$ RNA from 72 different human tissues and 8 different control RNAs and DNAs. The normalization was performed by the Clontech method. To account for differences in transcription levels, this method normalizes the loading on the MTE array by use of eight housekeeping genes (β-actin, glyceraldehyde 3-phosphate dehydrogenase, ubiquitin, 23-kDa highly basic protein, α-tubulin; phospholipase A2, ribosomal protein S9, transferrin receptor, and hypoxanthine guanine phosphoribosyl transferase) because they show minimal variation in all of the dots and also belong to different functional classes. Therefore, the values obtained from the Northern dots indicated the relative abundance of the target mRNAs in different tissues. The MTE was first incubated with anti-IDX riboprobe and quantified; this riboprobe was then stripped out, and the second probe (anti-E4A) was assayed. Other data are given in Supplemental Table 1.

Results

p19 mRNA Is Stable in Mammalian Cells and Is as Abundant as p21 mRNA in HeLa Cells. In previous experiments, we realized that the p19 mRNA was easily detected by RT-PCR (see Supplemental Fig. 1). We therefore quantified the relative abundance of the p21 *versus* the p19 mRNAs by a T1 RNase protection assay. This quantification assay using total HeLa RNA was performed with a human riboprobe designed to produce, after RNase T1 digestion, two protected fragments of 157 and 125 nt, whose intensities were directly proportional to the abundance of the p19 and p21 mRNAs, respectively. Densitometric analysis of *Lane 1* in Fig. 2*A* showed that the expected fragments protected from RNase T1 digestion, corresponding, respectively, to the p19 and p21 mRNAs were detected with the same abundance.

There are numerous studies on p21 mRNA in which the p19 mRNA was never detected or quantified. *A priori*, we presumed that in Northern blot assays both mRNAs would migrate to the same extent because they differ only in 82 nt. To test this, we performed exonic Northern assays with two specific antisense riboprobes: one complementary to the IDX sequence to detect the p19 mRNA, and a second probe complementary to the E4A exon to detect both the p19 and p21 mRNAs. As shown in *Lanes 1* and *2* in Fig. 2*B*, both antisense riboprobes labeled only one band. We further assessed the relative abundance of the p19 and p21 mRNAs by performing an exonic Northern dot blot assay on a multiple tissue array that contained mRNAs from different human tissues and cultured cell lines. In this assay, we used the same Northern antisense riboprobes. As shown in Fig. 2*C* (with anti-IDX riboprobe), the p19 mRNA was distinctly and stably expressed in all 72 human tissues and cell lines analyzed. The quantification of these Northern dot blot assays is shown in Supplemental Table 1. The highest relative abundances of p19 mRNA *versus* H-Ras (p19+p21) mRNA were in the following human tissues: ascending colon (80%; Fig. 2*C*, *dot 5H*); trachea (75%; Fig. 2*C*, *dot 7H*); fetal thymus (78%; Fig. 2*C*, *dot 11F*) and fetal lung (66%; Fig. 2*C*, *dot 11G*). Among human cell lines, those showing the highest relative abundances of p19 mRNA were as follows: Raji (70%; Fig. 2*C*, *dot 10E*); Daudi (71%; Fig. 2*C*, *dot 10F*); SW480 (74%; Fig. 2*C*, *dot 10G*), and A549 (81%; Fig. 2*C*, *dot 10H*). It should be noted that the value obtained for HeLa cells by the exonic Northern dot blot assay (52%; Fig. 2*C*, *dot 10B)* was similar to that obtained from the quantification by the RNase T1 protection assay (50%; see Fig. 2*A*). Tissues that showed smaller relative abundances of the p19 mRNA were bone marrow (30%; Fig. 2*C*, *dot 7G*) and pancreas (28%; Fig. 2*C*, *dot 9B*).

The IDX sequence is known to be conserved in the H-*ras* gene in rats and humans (4). We searched GenBank for genomic sequences containing E3-D intron-E4A of c-H-*ras* gene and found the human (GenBank accession no. J00277), hamster (GenBank accession no. M84166), mouse (GenBank accession no. AF081118) and rat (4) IDX sequences. An identical IDX sequence was also found in five human ESTs: GenBank accession no. AW269956.1 (from a mixed library from fetal lung, testis, and B cells); GenBank accession no. BE710671.1 (head and neck); GenBank accession no. F01147 (skeletal muscle); GenBank accession no. AI684659.1 (pooled tissues), and GenBank accession no. BC006499 (lung). Additionally, we amplified the region encompassing E3-E4A of the c-H-*ras* gene by RT-PCR using liver total RNA from cow, monkey, pig, and rabbit. Later, we also found a pig (identical to the one sequenced *de novo* by us) and a rat EST in GenBank, both containing the IDX sequence (GenBank accession nos. BG384594.1 and BG373388, respectively). The amplified bands were sequenced and aligned as shown in Fig. 2*D*. All of the sequences aligned come from mRNAs either amplified and sequenced by us or from reported ESTs. When we amplified cDNA from chicken, using primers specific for the chicken E3 and E4A c-H-*ras*, we detected only the p21 mRNA (not shown), suggesting that the p19 mRNA is not present in avians. It was also reported that this mRNA is not present in *Teleostei* (16); it therefore appears that the alternative splicing of the c-H-*ras* is limited to mammals.

The rat and mouse IDX nucleotide sequences in genomic, EST, and mRNA databanks present some interesting differences. This observation led us to sequence (in three independent experiments) the plus and minus strands of the IDX region of the p19 mRNA obtained from Rat-1 (rat) and NIH/3T3 (mouse) cells. The sequence of rat IDX, sequenced *de novo*, was identical to that reported previously (Ref. 4; Fig. 2*D*, *Rat sequence*) but not identical to the one described in GenBank (accession no. M13011; Ref. 17). The *de novo* IDX sequence of NIH/3T3 cell line (Fig. 2*D*, *Mouse 3 sequence*) differs considerably from that reported by Przybojewska and Plucienniczak (Ref. 18; GenBank accession no. Z50013) but is almost identical to

that reported by Esteban and Santos (GenBank accession no. AF081118; Fig. 2*D*, *Mouse 1 sequence*) and to a mouse EST sequence (GenBank accession no. BI731283.1; Fig. 2*D*, *Mouse 2 sequence*). The *de novo* NIH/3T3 IDX sequence contains a G instead of an A nucleotide at position 38, a change that has consequences in the amino acid translation (see below). The alignment in Fig. 2*D* shows that the IDX sequences and the position of the stop codon in frame with the amino acids that arise from E1-E3 translation are highly conserved in all of the species analyzed except for the mouse. The mouse IDX sequence is more divergent and does not include an in-frame stop codon, leading to significant changes in the length and amino acid composition of a putative mouse p19 protein. A previous study has shown that amino acids translated from IDX sequences from rat and human cDNA are conserved (4). Fig. 3*A* presents the translation of the IDX nucleotide sequence of all of the species analyzed. The 20-amino acid peptide at the COOH terminus, with a consensus sequence of GSRSGSGSSSGTLWDPPGPM, is well conserved in all species, which present only some point mutations and, in the case of the mouse sequence, two amino acid deletions. This peptide consensus sequence possesses a polar NH_2-terminal region rich in Gly and Ser residues and a hydrophobic COOH terminus rich in Pro residues.

As indicated above, the mouse IDX does not contain an in-frame stop codon, which is, however, present at nucleotide 33 of the E4A exon, downstream of the IDX sequence. Therefore, the COOH terminus of the mouse p19 protein contains 20 additional amino acids fused to the 18 NH_2-terminal IDX amino acids. Because of the different reading frame, the additional amino acids translated from E4A in the mouse p19 protein are different from those translated from the same exon in the mouse p21 protein (Fig. 3*A*, *Mouse EST*). As indicated above, the *de novo* sequenced IDX from NIH/3T3 cDNA (Fig. 3*A*, *Mouse3*) yields almost the same protein sequence as the mouse 1 and mouse 2 sequences, with the only difference being a Gly instead of an Asp at position 13 (Fig. 3*A*).

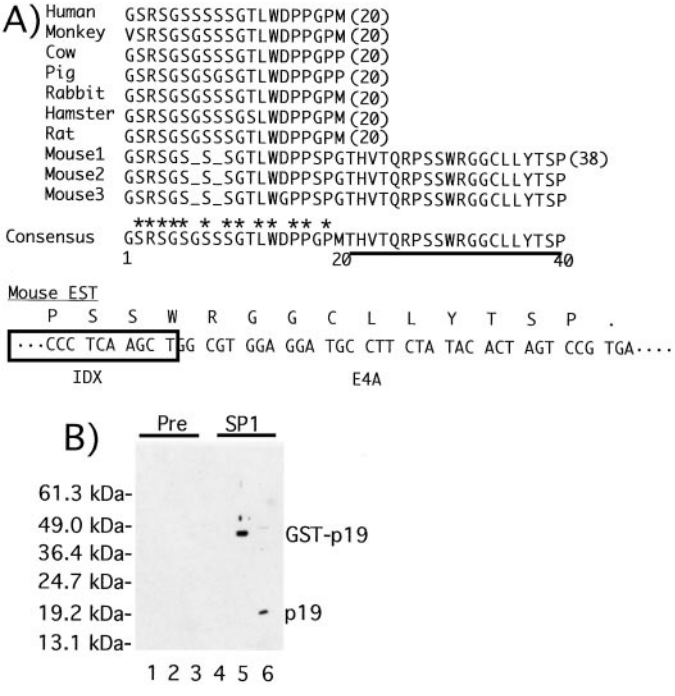

Fig. 3. p19 is expressed in mammalian cells. *A*, the amino acid sequences obtained from the translation of the IDX sequences and aligned with the MacMolly Tetra program (version 3.8) are shown. The 20 additional COOH-terminal residues (from 21 to 30 in mouse sequences) present only in mouse p19 are *underlined*. In the consensus sequence, which contains the most conserved residues in each position, the invariant amino acids are marked with ∗. *B*, Western blot with SP1 serum. *Lanes 3* and *6* contain proteins from a HeLa total SDS extract; *Lanes 2* and *5* contain protein from a total bacterial extract expressing GST-p19 recombinant protein; *Lanes 1* and *4* contain protein from a total bacterial extract expressing GST-p21 recombinant protein. *Lanes 1–3* were incubated with preimmune serum, and *Lanes 4–6* were incubated with the SP1 serum. Similar amounts of GST-p21 and GST-p19 were loaded in the corresponding lanes. GST-p19 and GST-p21 have molecular masses of 45 and 47 kDa, respectively. The faint band around 50 kDa in *Lane 6* is not detected with the immunoaffinity-purified antibodies (see Supplemental Fig. 2). The p19 protein has the new GenBank accession no. AJ437024.

p19 Protein Is Expressed in Human Cells. To determine whether the polyadenylated p19 mRNA is translated to protein in human cells, we raised polyclonal specific antibodies directed against the GSRSGSSSSSGTLWD peptide, which corresponds to the COOH terminus of the hypothetical human p19 protein. This peptide does not show any significant homology to known rabbit or human proteins. One reacting serum, named SP1, was obtained, which recognized the GSRSGSSSSSGTLWD peptide by ELISA (data not shown) and a GST-p19 recombinant protein by Western blot (Fig. 3*C*, *Lane 5*), whereas it did not recognize the negative control GST-p21 recombinant protein (Fig. 3*B*, *Lane 4)*. Furthermore, in a total extract from HeLa cells, the antiserum detected a band with the expected molecular mass of 19 kDa (Fig. 3*B*, *Lane 6*), indicating that the p19 protein is expressed in this cell line. A polyclonal anti-p21 specific antibody (C-20; Santa Cruz Biotechnology) did not recognize either the GST-p19 fusion protein or the p19 protein (not shown).

Human p19 Protein Localizes in Both the Nucleus and the Cytoplasm. To study the subcellular distribution of the p19 protein, we transiently transfected COS-1 and HeLa cells with a plasmid coding for GFP fused to the NH_2 terminus of the full-length p19. As controls, the plasmids coding for the GFP-p21 fusion protein and for GFP alone (pEGFP-C1) were also transfected.

GFP-p21 localized in plasma membrane and also decorated the Golgi apparatus (Fig. 4, *A–C*) in COS-1 and HeLa cells, as reported previously (19, 20). The subcellular distribution of the transiently expressed GFP-p19 protein was different in COS-1 and HeLa cells. Some COS-1 cells showed nuclear and cytoplasmic fluorescence (Fig. 4*D*); however, in the vast majority of the cells, the GFP-p19 fluorescence was found almost exclusively in the cytoplasm (Fig. 4*E*). HeLa cells expressing GFP-p19 displayed a more heterogeneous pattern. A large number of cells exhibited uniform staining of both the nucleus and the cytoplasm (not shown), but some cells presented either diffuse or speckled nuclear fluorescence (Fig. 4, *F* and *G*). GFP alone was distributed between the nucleus and the cytoplasm of the transfected cells, although the fluorescence intensity in the nucleus was slightly higher (not shown).

The subcellular distribution of p19 was further studied in two ways. First, we deleted the GFP nucleotide sequence from the GFP-p19 plasmid. The plasmid thus generated, named (ΔGFP)p19, was used to transiently express the p19 protein alone, which was then detected by indirect IF. Second, we also analyzed the distribution of endogenous p19 by IF. Because the crude SP1 serum showed very faint indirect immunostaining of HeLa or COS-1 cells (not shown), anti-p19 antibodies were purified from this serum by affinity chromatography using the GSRSGSSSSSGTLWD peptide covalently bound to Sepharose beads. The purified antibodies specifically recognized the GSRSGSSSSSGTLWD peptide in ELISAs and the GST-p19 recombinant protein by Western blot analysis (not shown). Furthermore, these antibodies detected endogenous p19 in a nuclear extract from HeLa cells, thus providing additional evidence of the nuclear localization of this protein (see the Western blot in Supplemental Fig. 2).

COS-1 cells transfected with the (ΔGFP)p19 plasmid showed nuclear and cytoplasmic fluorescence, but in many cases the intensity of fluorescence was higher in the nuclei, in which it presented either diffuse or speckled patterns (Fig. 4, *I* and *J*). IF detection of the endogenous p19 protein with the immunopurified SP1 antibodies gave faint fluorescence, which concentrated in the nucleus of COS-1 cells

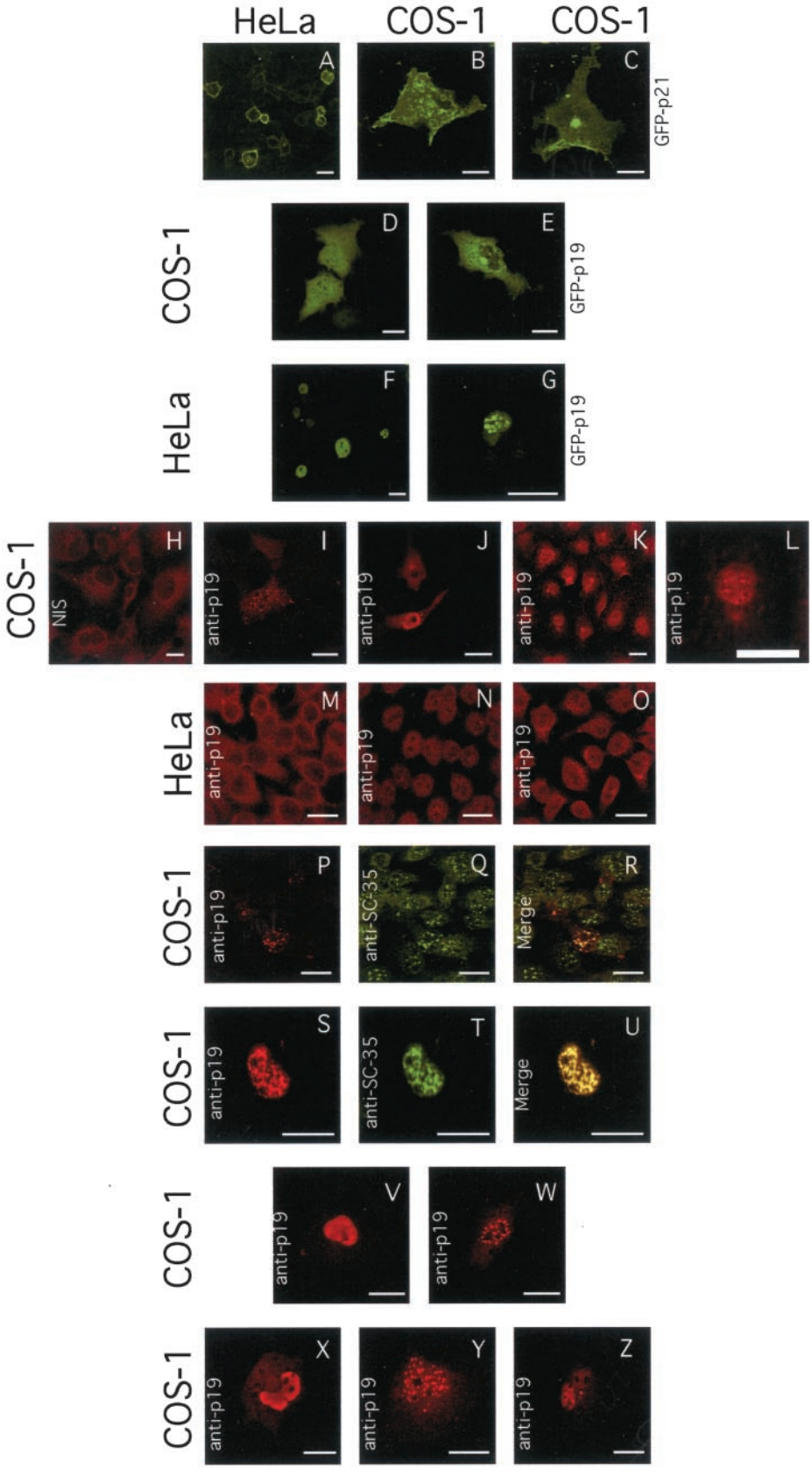

Fig. 4. Subcellular distribution of p19 in COS-1 and HeLa cells. Cell types are listed *above* (for a panel) or on the *left* (for a line of panels). *Panels A–G* are confocal microscope images of cells that transiently express GFP-p21 (*A–C*) or GFP-p19 (*D–G*). *Panels H* and *M* show IF detection of COS-1 or HeLa cells, respectively, transiently transfected with the (ΔGFP)-p19 plasmid and incubated with the preimmune serum (1:50 dilution). Nontransfected cells showed the same results as seen in *panels H* and *M*. *Panels I*, *J*, and *N* show IF detection of cells transiently transfected with the (ΔGFP)-p19 plasmid and stained with immunopurified SP1 antibodies (1:50 dilution). *Panels K* and *O* show IF detection of endogenous p19 in COS-1 or HeLa cells, respectively, with immunopurified SP1 antibodies (1:10 dilution). *Panel L* is similar as *panel K*, but showing a COS-1 cell with speckles. *Panels P* and *S* show the IF detection of COS-1 cells transfected with the (ΔGFP)-p19 plasmid and incubated with immunopurified SP1 antibodies (1:50 dilution). *Panels Q* and *T* show IF detection of endogenous SC-35 with a mouse anti-SC-35 antibody (1:50 dilution), and *panels R* and *U* show overlapped fluorescence images of the corresponding previous panels. *Panels X–Z* show IF detection with immunopurified SP1 antibodies (1:50 dilution) of COS-1 cells transiently expressing the Gly12Val (*panel Z*) and Ser17Arg (*panels X* and *Y*) mutants of p19. The Gly12Val mutant also presented a nuclear speckled pattern (not shown). For comparison, *panels V* and *W* show IF detection of cells transiently expressing the wild-type p19 protein. Rabbit and mouse primary antibodies were detected with Texas red-labeled (TRITC) anti-rabbit or fluorescein-labeled (FITC) anti-mouse secondary antibodies, respectively. *Red*, fluorescence from TRITC-labeled secondary antibodies; *green*, fluorescence from transiently expressed GFP proteins (*panels A–G*) or from FTIC-labeled secondary antibodies (*panels Q* and *T*); *yellow*, colocalization of the TRITC- and FITC-conjugated secondary antibodies (*panels R* and *U*). *Bars*, 20 μm.

(Fig. 4*K*), and some cells showed a faint speckled pattern (Fig. 4*L*). Similar results were obtained with HeLa cells, which showed mainly nuclear fluorescence in the (ΔGFP)p19 transfected cells (Fig. 4*N*). The IF detection of endogenous p19 protein also yielded a faint staining, which concentrated in the nuclear compartment (Fig. 4*O*). To characterize the nature of the speckles observed with the transiently expressed p19 protein, we analyzed (using confocal microscopy) whether this protein colocalized with several nuclear markers in

COS-1 cells. The antinuclear antibodies used mapped specific nuclear structures or factors that displayed a speckled pattern, such as UsnRNPs, centromeres, nucleoli, p-80 coilin, and SC-35. This analysis showed that SC-35, a non-UsnRNP protein of the spliceosome that is a marker of the IGCs (21), was the only antigen tested that colocalized with p19 (Fig. 4, *P–U*). The colocalization was transient because for some cells we observed no colocalization at all (not shown), whereas in others, only a subset of the speckles containing the SC-35 antigen also contained p19 (Fig. 4*R*). In addition, in some cells all of the nuclear speckles that were labeled with anti-p19 antibodies were also stained with the anti-SC-35 antibodies (Fig. 4*U*). The altered subcellular location of p19 is not surprising and is expected because p19 lacks the COOH-terminal CAAX motif and hence is not posttranslationally modified by farnesylation, a key modification needed for membrane targeting.

Several mutations of p21 have been described in tumor cells that correlate with a higher transforming activity of the H-*ras* gene. Any mutation within the E1–E3 exons of the H-*ras* gene will simultaneously affect p21 and p19 sequences and potentially affect the function of both proteins. One of these mutations, at codon 12 of the H-*ras* gene (mut12), has been shown to activate p21 by locking the protein in its GTP-bound active state (reviewed in Refs. 1–3). A recent report showed that a transiently expressed Gly12Val mutant of p21 presented a nuclear localization when cotransfected with a mutant of p53 (22). Another mutant, the Ser17Arg variant, has been described as a dominant-negative form of p21 protein (23). When assessing the presence of GTPases in IGCs, we found that the GTPase RagA is localized in cytoplasm; however, its dominant-negative mutant is distributed in the nucleus, colocalizing with SC-35 (IGCs; Ref. 24). Furthermore, the RagA dominant-positive mutant localizes in cytoplasm (24). The findings in the latter study on RagA that p19 also localizes in the nucleus, IGCs, and cytoplasm (24) prompted us, as an initial approach, to check whether some of the reported H-*ras* mutations alter the subcellular distribution of the p19 protein. Two plasmids encoding Gly12Val and Ser17Arg mutants of p19 were transiently transfected in COS-1 cells, and the subcellular distribution of the mutant proteins was analyzed by IF. Both mutants showed distribution identical to that of wild-type p19 protein and presented either nuclear diffuse or speckled patterns (Fig. 4, *V–Z*).

We next investigated whether p19 is a biologically active protein. To answer this question, we first ascertained whether p19 has GTP-binding activity and then screened a human cDNA library, by yeast two-hybrid assay, using p19 sequence as a bait.

p19 GTP-binding Activity. We obtained pure recombinant GST, GST-p21, and GST-p19 and allowed these proteins to bind to [γ-^{32}P]GTP. Slot blots and quantification of data (Fig. 5) showed that GST-p19 has a GTP-binding activity similar to background values (GST alone). These latter GTP-binding results and the ones described above, showing that p19 protein does not concentrate in plasmatic membranes, indicate that the p19 protein probably does not interact with most of the p21 effectors. To address this question, we studied the binding of Raf1 and Rin1 (p21 effectors) to p19 protein by yeast two-hybrid assays. As can be seen in Fig. 5*B*, Raf1 and Rin1 did not interact with p19 under the same conditions as they did with p21. Furthermore, screenings of cDNA libraries by yeast two-hybrid assays with p19 sequence as a bait did not select Raf1, Rin1, phosphatidylinositol 3-kinase, or RalGDS (see below). The results of this assay also indicated that p19 protein may interact with itself.

p19 Protein Interacts with the RACK1 Scaffolding Protein. The plasmid pGBKT7-p19 was the bait used for the screening of a pretransformed liver human cDNA library (cloned in pACT2 vector; Clontech) by yeast two-hybrid assay. This cDNA yeast library was obtained from a previous bacteria cDNA library with at least 1×10^6 independent clones. Following the manufacturer's instructions, we obtained by mating 3×10^6 yeast diploid colonies that grow in −Leu/−Trp/−His/−Ade selective medium. After exhaustive functional assays of the clones obtained with nonrelated proteins to eliminate nonspecific binding, we obtained a clone with a sequence encoding RACK1, a protein that specifically interacted with p19 protein. We did not obtain the sequence of Ral-GDS or phosphatidylinositol 3-kinase effectors from these screenings, which is consistent with the results for the Rin1 and Raf1 effectors as described above in Fig. 5*B*.

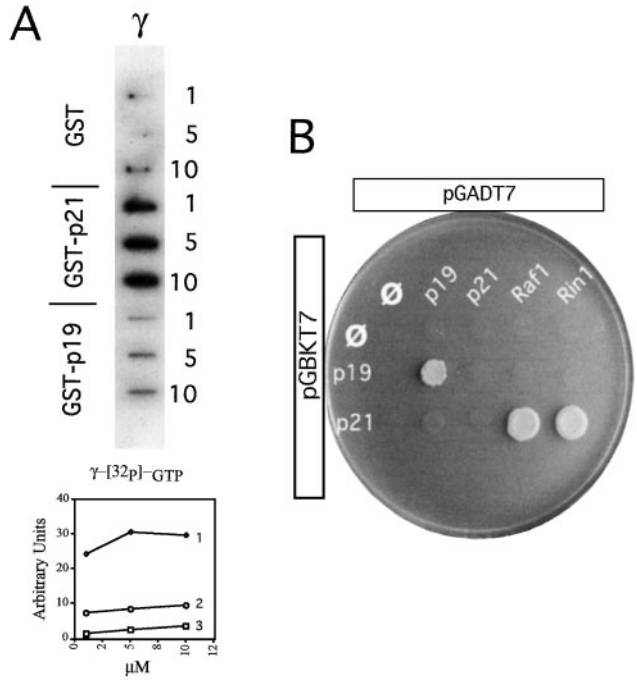

Fig. 5. Functional assays of p19. *A*, GTP-binding assay. Slot blot showing the GTP-binding activity between recombinant GST, GST-p19, and GST-p21 proteins and the nucleotides [γ-^{32}P]GTP (5000 Ci/mmol). The molarity of the proteins during the assay is stated (1, 5, and 10 μM) to the *right* of the slot blot; γ-GTP concentration, 0.05 μM. The quantification results for the slot blot are shown in the graph *below* the slot blot. Autoradiographs were scanned with a Molecular Dynamics laser densitometer, and the internal integration was used to determine peak areas with the ImageQuant program: *line 1*, GST-p21; *line 2*, GST-p19; *line 3*, GST. *B*, yeast two-hybrid assay for the binding potential of p19 with known p21 effectors. Shown is yeast strain AH109, coexpressing GAL4 DNA BD alone (*row Ø*), fused to p19 (*row p19*), or fused to p21 (*row p21*) and GAL4 AD fused to p19 (*column p19*), p21 (*column p21*), Raf1 (*column Raf1*), or Rin1 (*column Rin1*) or alone (*column Ø*). An aliquot of a saturated culture of each cotransformed strain was seeded on a −Leu/−Trp/−His/−Ade plate and documented after incubation for 5 days at 30°C.

RACK1 is a scaffolding protein that interacts with numerous proteins (including PKC), several of which are linked to G-protein signaling (25). Additionally, RACK1 is also a trafficking protein; thus, it can be detected in many cellular compartments, including the nucleus (25). p19-RACK1 binding was further validated by colocalization during immunodetection with specific antibodies (anti-p19 and anti-RACK1) and GST pull-down assays. As shown in Fig. 6, endogenous RACK1 and p19 colocalize in the perinuclear region (Fig. 6*A*, *panel MERGE*) and GST-p19 pulls down endogenous RACK1 (see Fig. 6*B*, *Lane 2*; compare with *Lanes 1* and *3*). GST-p21 also showed some RACK1-binding activity (compare *Lanes 1* and *3* in Fig. 6*B*), but that activity was lower than the activity for GST-p19. This suggests that the amino acids encoded by the IDX exon could have a direct role in the binding of p19 to RACK1. To assess this, we compared, using several Internet proteomic softwares, the between of IDX and other protein domains. Interestingly, we observed that IDX amino acids display some similarities to a domain described previ-

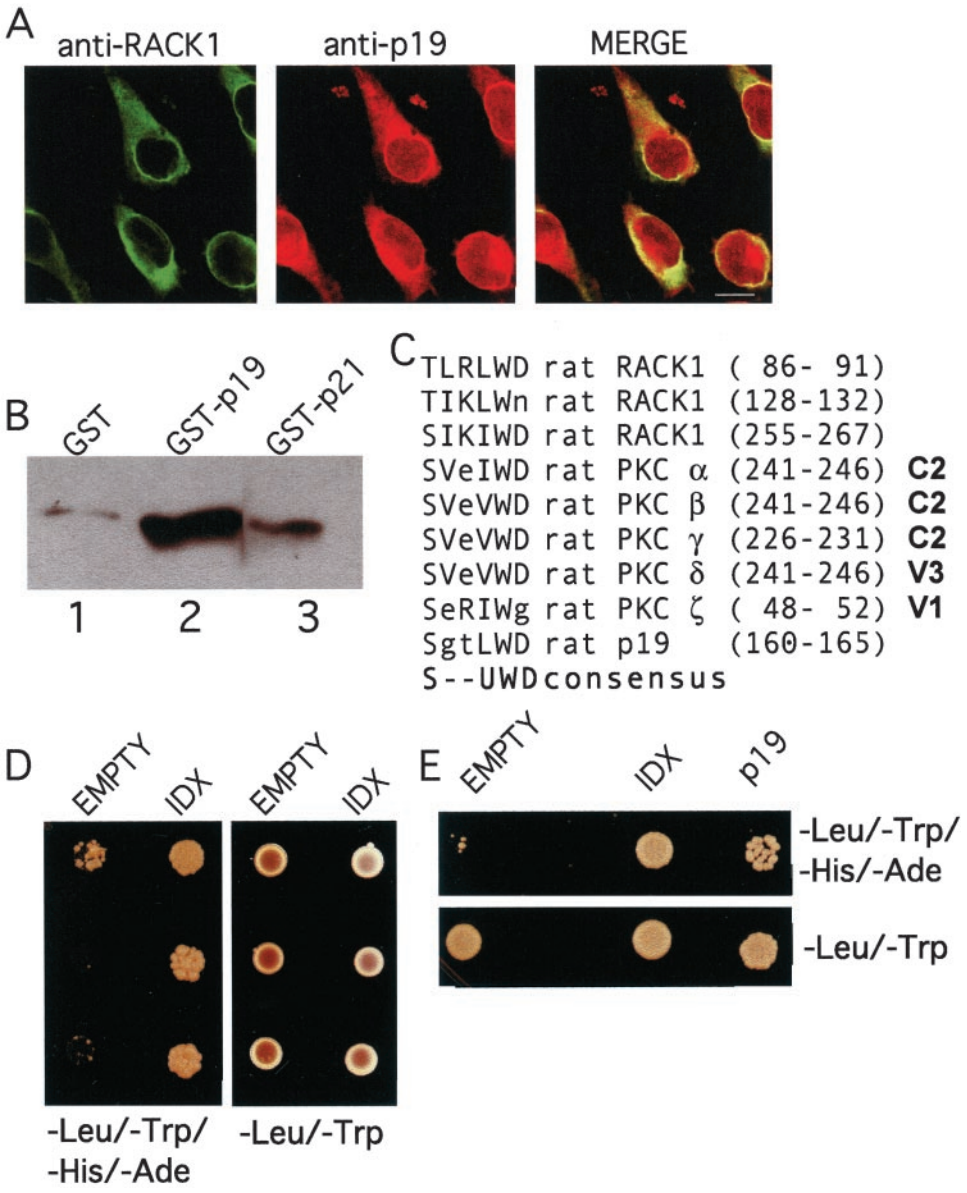

Fig. 6. p19 interacts with RACK1, a scaffolding protein. *A*, co-immunolocalization of RACK-1 and p19 in HeLa cells. Assay was performed on endogenous proteins as described in Fig. 4. Anti-Rack antibody (IgM mouse antibody; clone 20) was obtained from BD Biosciences and diluted 1:1000. *Bar*, 8 μm. *B*, GST pull-downs were performed essentially as described previously (52), with 4 nmols each of GST (*Lane 1*), GST-p19 (*Lane 2*), and GST-p21 (*Lane 3*) bound to GSTrap resin (Pharmacia) and incubated with 300 μl of CHAPS/MOPS total extract (53). The final Western blot was incubated with anti-RACK1 antibody diluted 1:500. The *blot* shows the RACK1 protein pulled-down with the same nanomoles of the three proteins tested. *C*, sequence similarities between RACK1, PKCs, and p19 according to Ron *et al.* (26). *C2* is the region of PKCs found to contain at least part of the RACK binding site on PKCs. *U* in the consensus sequence indicates an uncharged amino acid. *D* and *E*, yeast two-hybrid assay performed between pGBKT7-empty vector (*EMPTY*), pGBKT7-IDX (*IDX*) or pGBKT7-p19 (*p19*) *versus* pACT2-RACK1 (in *all columns*). The −Leu/−Trp plates act as the positive controls for growth and/or number of yeast cells of the corresponding −Leu/−Trp/−His/−Ade plates.

ously for RACK1 and PKC (26). This domain is shown in Fig. 6*C* (rat sequences) and is compared with the rat p19 region. Furthermore, this domain was suggested to have a dual function: it could be a "pseudo-RACK1"-binding site (26) and is also present in the C2 region of PKC (see Fig. 6*C*), which was previously found to contain at least part of the RACK-binding site on PKC (27). This observation indicates that the SgtLWD in p19 protein may mimic the RACK1-binding site in the C2 PKC region, suggesting that some IDX amino acids may interact with RACK1. To further demonstrate the presence of this putative binding site, we performed a yeast two-hybrid assay using the human IDX amino acids only as a bait *versus* RACK1 protein. As shown in Fig. 6*D* (with three different clones from the yeast transformation plate), the IDX amino acids interact only with RACK1 protein. We also observed that RACK1 consistently interacted more strongly with IDX amino acids than with wild-type 19 protein in yeast two-hybrid assays (one example is shown in Fig. 6*E*; compare IDX with p19). This observation indicates that IDX amino acids in the wild-type p19 protein are not as free to interact with RACK1 and suggests that amino acids encoded by exons E1–E3 may regulate p19-RACK1 binding.

Discussion

In this study, we have shown that p19 mRNA is stable and quite abundant in several cell lines and human tissues. We also detected the protein resulting from the translation of the p19 mRNA. Furthermore, we have shown that this protein does not accumulate in the plasma membrane but is distributed between the cytosol and the nucleus of HeLa and COS-1 cells. An important conclusion of our work is that any mutation within exons E1–E3 of the H-*ras* gene will simultaneously affect the amino acid sequences of p21 and p19 proteins. Therefore, any altered cellular function that results from this type of mutation cannot be directly and exclusively attributed to p21 because it may be caused by an alteration of p19 function.

The nuclear, diffuse or speckled, and cytoplasmic localization of the p19 protein constitutes a significant difference between the p19 protein and the other four members of the Ras family. Our observations indicate that p19 trafficks through the nucleoplasma, IGCs, and cytoplasm. The IGCs have been associated with the pre-mRNA maturation processes (28, 29). The transient colocalization of p19 with IGCs suggests a function for p19 in pre-mRNA maturation or mRNA

movement from active chromatin to the splicing machinery and mRNA export (30). The p19 protein did not colocalize with UsnRNPs or markers of coiled bodies, which are found in active splicing sites. However, these observations do not exclude a splicing function for p19 because IGCs contain many splicing factors, such as the SR proteins (31).

The clearly diminished GTP-binding activity of p19 in comparison with p21 was expected, and had been reported in 1989 (4), because p19 lacks two important GTP-binding sites located in E4A of the p21 protein. Furthermore, in 1986, it was already shown that the mutation of the Arg164 residue (inside E4A) of p21 renders a protein that has lost its GTP-binding activity (32). Previous results suggested that p19 could be an inhibitory factor of transforming p21 (5). This led us to test whether p19 could interfere with the binding between p21 and two of its downstream effectors, Raf1 and Rin1. The results indicating the absence of interactions between p19 and these effectors, together with the GTP-binding assays, indicate that although all of the sequences required to interact with the effectors are retained in p19, they are not accessible to Raf1 or Rin1. Hence, the "p21-GTP active stage" is not achieved in p19 in the presence of GTP. In addition, p19 did not interact with p21 in the yeast two-hybrid assays but was able to interact with itself, suggesting that this protein may dimerize. This process is reminiscent of the dimerization of the p21 protein at the plasma membrane (33). Thus, to really define p19 as a protein that interferes with the binding between p21 and other factors, we need to identify a common p21- and p19-binding protein. Could the RACK1 protein be this link? From our work, it is yet not possible to definitely conclude this. To date, RACK1 has not been described as a p21-binding protein, although RACK1 displayed some p21-binding activity in our pull-down assays (Fig. 6*B*), an interaction that was also seen in yeast two-hybrid assays (not shown). RACK1 has also been found to be associated with the plasma membrane (25). Additionally, RACK1 is a WD40 repeat protein and was initially described as being able to bind to and localize with activated βIIPKC (34, 35). Moreover, RACK1 has been shown to interact with several important proteins, such as dynamin-1 (36); Src (37, 38); the β subunit of integrins (39, 40); p120GAP (41); PDE4D5 (42, 43); the IFN-α receptor (44); the β chain of interleukin-5 receptor (45); the protein-tyrosine phosphatase PTPμ (46); the $\beta\gamma$-subunit of heterotrimeric G proteins (47); the NR2B subunit of the *N*-methyl-D-aspartate receptor; the nonreceptor protein tyrosine kinase, Fyn (48); the factor associated with neutral sphingomyelinase activation (49); the stress-induced splice variant of acetylcholinesterase, AChE-R (50); and insulin-like growth factor 1 receptor (51). RACK1 is a scaffolding protein that allows specific multiprotein complexes to form during different signaling events. The binding of p19 to RACK1 initially links the c-H-*ras* gene to protein multicomplexes (and associates p19 to the above-described RACK1-binding proteins) recruited by RACK1 to participate in one specific signaling pathway. Additionally, it demonstrates that p19 is a biologically active protein. Studies on whether the interaction of p19 with RACK1 is exclusive or concurrent with any of the other RACK1-binding proteins will render more information about the specific p19 signaling pathway.

The regulation of the Ras activity by alternative splicing of COOH-terminal exons is not new in the Ras family. The K-*ras* gene also renders two proteins (K-Ras4A and K-Ras4B) by alternative splicing of the last encoding exons, 4A and 4B, which display differential trafficking and localization in the plasma membrane (reviewed in Ref. 1). The c-H-*ras* proto-oncogene is therefore the second member of the Ras family that multiplies its genetic potential by rendering two proteins that present differential subcellular localization and presumably have distinct roles that complement each other to completely express the functional information encoded by the H-*ras* gene. p19 represents a new example of how the transcriptosome or the RNA factory amplifies and modulates the genetic information.

Acknowledgments

We thank Dr. Ruth Willmott for revising the manuscript.

References

1. Reuther, G. W., and Der, C. J. The Ras branch of small GTPases: Ras family members don't fall far from the tree. Curr. Opin. Cell. Biol., *12:* 157–165, 2000.
2. Barbacid, M. *ras* genes. Annu. Rev. Biochem., *56:* 779–827, 1987.
3. Malumbres, M., and Pellicer, A. RAS pathways to cell cycle control and cell transformation. Front. Biosci., *3:* d887–912, 1998.
4. Cohen, J. B., Broz, S. D., and Levinson, A. D. Expression of the H-ras proto-oncogene is controlled by alternative splicing. Cell, *58:* 461–472, 1989.
5. Huang, M. Y., and Cohen, J. B. The alternative H-ras protein p19 displays properties of a negative regulator of p21Ras. Oncol. Res., *9:* 611–621, 1997.
6. Guil, S., Gattoni, R., Carrascal, M., Abián, J., Stévenin, J., and Bach-Elias, M. Roles of hnRNP A1, SR proteins, and p68 helicase in c-H-ras alternative splicing regulation. Mol. Cell. Biol., *23:* 2927–2941, 2003.
7. De la Iglesia, N., Veiga-da-Cunha, M., Van Schaftingen, E., Guinovart, J. J., and Ferrer, J. C. Glucokinase regulatory protein is essential for the proper subcellular localisation of liver glucokinase. FEBS Lett., *456:* 332–338, 1999.
8. Glisin, V., Crkvenjakov, R., and Byus, C. Ribonucleic acid isolated by cesium chloride centrifugation. Biochemistry, *13:* 2633–2637, 1974.
9. Dignam, J. D., Lebovitz, R. M., and Roeder, R. G. Accurate transcription initiation by RNA polymerase II in a soluble extract from isolated mammalian nuclei. Nucleic Acids Res., *11:* 1475–1489, 1983.
10. Bahia, D., Font, J., Khaouja, A., Carreras, N., Espuny, R., Cicarelli, R. M. B., Ingelmo, M., and Bach-Elias, M. Antibodies to yeast Sm motif 1 cross-react with human Sm core polypeptides. Eur. J. Biochem., *261:* 371–378, 1999.
11. Kaelin, W. G., Jr., Krek, W., Sellers, W. R., DeCaprio, J. A., Ajchenbaum, F., Fuchs, C. S., Chittenden, T., Li, Y., Farnham, P. J., Blanar, M. A., *et al.* Expression cloning of a cDNA encoding a retinoblastoma-binding protein with E2F-like properties. Cell, *70:* 351–364, 1992.
12. Kaur, K. J., and White, M. A. Isolation of effector-selective Ras mutants by yeast two-hybrid screening. Methods Enzymol., *332:* 270–277, 2001.
13. Pieper, U., Brinkmann, T., Kruger, T., Noyer-Weidner, M., and Pingoud, A. Characterization of the interaction between the restriction endonuclease McrBC from *E. coli* and its cofactor GTP. J. Mol. Biol., *272:* 190–199, 1997.
14. Codony, C., Guil, S., Caudevilla, C., Serra, D., Asins, G., Graessmann, A., Hegardt, F. G., and Bach-Elias, M. Modulation *in vitro* of H-ras oncogene expression by trans-splicing. Oncogene, *20:* 3683–3694, 2001.
15. Porchet, N., and Aubert, J. P. Northern blot analysis of large mRNAs. Methods Mol. Biol., *125:* 305–312, 2000.
16. Lee, J. S., Choe, J., and Park, E. H. Absence of the intron-D-exon of c-Ha-ras oncogene in the hermaphroditic fish *Rivulus marmoratus* (Teleostei: *Rivulidae*). Biochem. Mol. Biol. Int., *34:* 921–926, 1994.
17. Ruta, M., Wolford, R., Dhar, R., Defeo-Jones, D., Ellis, R. W., and Scolnick, E. M. Nucleotide sequence of the two rat cellular rasH genes. Mol. Cell. Biol., *6:* 1706–1710, 1986.
18. Przybojewska, B., and Plucienniczak, G. Nucleotide sequence of c-H-ras-1 gene from B6C3F1 mice. Acta Biochim. Pol., *43:* 575–578, 1996.
19. Apolloni, A., Prior, I. A., Lindsay, M., Parton, R. G., and Hancock, J. F. H-ras but not K-ras traffics to the plasma membrane through the exocytic pathway. Mol. Cell. Biol., *20:* 2475–2487, 2000.
20. Choy, E., Chiu, V. K., Silletti, J., Feoktistov, M., Morimoto, T., Michaelson, D., Ivanov, I. E., and Philips, M. R. Endomembrane trafficking of ras: the CAAX motif targets proteins to the ER and Golgi. Cell, *98:* 69–80, 1999.
21. Spector, D. L., Fu, X. D., and Maniatis, T. Associations between distinct pre-messenger RNA splicing components and the cell nucleus. EMBO J., *10:* 3467–3481, 1991.
22. Wurzer, G., Mosgoeller, W., Chabicovsky, M., Cerni, C., and Wesierska-Gadek, J. Nuclear Ras: unexpected subcellular distribution of oncogenic forms. J. Cell. Biochem., *81:* 1–11, 2001.
23. Feig, L. A., and Cooper, G. M. Inhibition of NIH 3T3 cell proliferation by a mutant ras protein with preferential affinity for GDP. Mol. Cell. Biol., *8:* 3235–3243, 1988.
24. Hirose, E., Nakashima, N., Sekiguchi, T., and Nishimoto, T. RagA is a functional homologue of *S. cerevisiae* Gtr1p involved in the Ran/Gsp1-GTPase pathway. J. Cell. Sci., *111:* 11–21, 1998.
25. Schechtman, D., and Mochly-Rosen, D. Adaptor proteins in protein kinase C-mediated signal transduction. Oncogene, *20:* 6339–6347, 2001.
26. Ron, D., Chen, C. H., Caldwell, J., Jamieson, L., Orr, E., and Mochly-Rosen, D. Cloning of an intracellular receptor for protein kinase C: a homolog of the β subunit of G proteins. Proc. Natl. Acad. Sci. USA, *91:* 839–843, 1994.
27. Smith, B. L., and Mochly-Rosen, D. Inhibition of protein kinase C function by injection of intracellular receptors for the enzyme. Biochem. Biophys. Res. Commun., *188:* 1235–1240, 1992.
28. Moen, P. T., Jr., Smith, K. P., and Lawrence, J. B. Compartmentalization of specific pre-mRNA metabolism: an emerging view. Hum. Mol. Genet., *4* (Spec No)*:* 1779–1789, 1995.
29. Stein, G. S., van Wijnen, A. J., Stein, J. L., Lian, J. B., Montecino, M., Choi, J., Zaidi, K., and Javed, A. Intranuclear trafficking of transcription factors: implications for biological control. J. Cell. Sci., *113* (Pt. 14)*:* 2527–2533, 2000.

30. Johnson, C., Primorac, D., McKinstry, M., McNeil, J., Rowe, D., and Lawrence, J. B. Tracking COL1A1 RNA in osteogenesis imperfecta: splice-defective transcripts initiate transport from the gene but are retained within the SC35 domain. J. Cell. Biol., *150:* 417–431, 2000.
31. Mintz, P. J., Patterson, S. D., Neuwald, A. F., Spahr, C. S., and Spector, D. L. Purification and biochemical characterization of interchromatin granule clusters. EMBO J., *18:* 4308–4320, 1999.
32. Lacal, J. C., Anderson, P. S., and Aaronson, S. A. Deletion mutants of Harvey ras p21 protein reveal the absolute requirement of at least two distant regions for GTP-binding and transforming activities. EMBO J., *5:* 679–687, 1986.
33. Inouye, K., Mizutani, S., Koide, H., and Kaziro, Y. Formation of the Ras dimer is essential for Raf-1 activation. J. Biol. Chem., *275:* 3737–3740, 2000.
34. Ron, D., and Mochly-Rosen, D. An autoregulatory region in protein kinase C: the pseudoanchoring site. Proc. Natl. Acad. Sci. USA, *92:* 492–496, 1995.
35. Stebbins, E. G., and Mochly-Rosen, D. Binding specificity for RACK1 resides in the V5 region of β II protein kinase C. J. Biol. Chem., *276:* 29644–29650, 2001.
36. Rodriguez, M. M., Ron, D., Touhara, K., Chen, C. H., and Mochly-Rosen, D. RACK1, a protein kinase C anchoring protein, coordinates the binding of activated protein kinase C and select pleckstrin homology domains in vitro. Biochemistry, *38:* 13787–13794, 1999.
37. Chang, B. Y., Chiang, M., and Cartwright, C. A. The interaction of Src and RACK1 is enhanced by activation of protein kinase C and tyrosine phosphorylation of RACK1. J. Biol. Chem., *276:* 20346–20356, 2001.
38. Chang, B. Y., Conroy, K. B., Machleder, E. M., and Cartwright, C. A. RACK1, a receptor for activated C kinase and a homolog of the β subunit of G proteins, inhibits activity of src tyrosine kinases and growth of NIH 3T3 cells. Mol. Cell. Biol., *18:* 3245–3256, 1998.
39. Buensuceso, C. S., Woodside, D., Huff, J. L., Plopper, G. E., and O'Toole, T. E. The WD protein Rack1 mediates protein kinase C and integrin-dependent cell migration. J. Cell Sci., *114:* 1691–1698, 2001.
40. Liliental, J., and Chang, D. D. Rack1, a receptor for activated protein kinase C, interacts with integrin β subunit. J. Biol. Chem., *273:* 2379–2383, 1998.
41. Koehler, J. A., and Moran, M. F. RACK1, a protein kinase C scaffolding protein, interacts with the PH domain of p120GAP. Biochem. Biophys. Res. Commun., *283:* 888–895, 2001.
42. Steele, M. R., McCahill, A., Thompson, D. S., MacKenzie, C., Isaacs, N. W., Houslay, M. D., and Bolger, G. B. Identification of a surface on the β-propeller protein RACK1 that interacts with the cAMP-specific phosphodiesterase PDE4D5. Cell. Signal., *13:* 507–513, 2001.
43. Yarwood, S. J., Steele, M. R., Scotland, G., Houslay, M. D., and Bolger, G. B. The RACK1 signaling scaffold protein selectively interacts with the cAMP-specific phosphodiesterase PDE4D5 isoform. J. Biol. Chem., *274:* 14909–14917, 1999.
44. Usacheva, A., Smith, R., Minshall, R., Baida, G., Seng, S., Croze, E., and Colamonici, O. The WD motif-containing protein receptor for activated protein kinase C (RACK1) is required for recruitment and activation of signal transducer and activator of transcription 1 through the type I interferon receptor. J. Biol. Chem., *276:* 22948–22953, 2001.
45. Geijsen, N., Spaargaren, M., Raaijmakers, J. A., Lammers, J. W., Koenderman, L., and Coffer, P. J. Association of RACK1 and PKCβ with the common β-chain of the IL-5/IL-3/GM-CSF receptor. Oncogene, *18:* 5126–5130, 1999.
46. Mourton, T., Hellberg, C. B., Burden-Gulley, S. M., Hinman, J., Rhee, A., and Brady-Kalnay, S. M. The PTPμ protein-tyrosine phosphatase binds and recruits the scaffolding protein RACK1 to cell-cell contacts. J. Biol. Chem., *276:* 14896–14901, 2001.
47. Dell, E. J., Connor, J., Chen, S., Stebbins, E. G., Skiba, N. P., Mochly-Rosen, D., and Hamm, H. E. The $\beta\gamma$ subunit of heterotrimeric G proteins interacts with RACK1 and two other WD repeat proteins. J. Biol. Chem., *277:* 49888–49895, 2002.
48. Yaka, R., Thornton, C., Vagts, A. J., Phamluong, K., Bonci, A., and Ron, D. NMDA receptor function is regulated by the inhibitory scaffolding protein, RACK1. Proc. Natl. Acad. Sci. USA, *99:* 5710–5715, 2002.
49. Tcherkasowa, A. E., Adam-Klages, S., Kruse, M. L., Wiegmann, K., Mathieu, S., Kolanus, W., Kronke, M., and Adam, D. Interaction with factor associated with neutral sphingomyelinase activation, a WD motif-containing protein, identifies receptor for activated C-kinase 1 as a novel component of the signaling pathways of the p55 TNF receptor. J. Immunol., *169:* 5161–5170, 2002.
50. Birikh, K. R., Sklan, E. H., Shoham, S., and Soreq, H. Interaction of "readthrough" acetylcholinesterase with RACK1 and PKCbeta II correlates with intensified fear-induced conflict behavior. Proc. Natl. Acad. Sci. USA, *100:* 283–288, 2003.
51. Kiely, P. A., Sant, A., and O'Connor, R. RACK1 is an insulin-like growth factor 1 (IGF-1) receptor-interacting protein that can regulate IGF-1-mediated Akt activation and protection from cell death. J. Biol. Chem., *277:* 22581–22589, 2002.
52. Vojtek, A. B., Hollenberg, S. M., and Cooper, J. A. Mammalian Ras interacts directly with the serine/threonine kinase Raf. Cell, *74:* 205–214, 1993.
53. Hamilton, M., and Wolfman, A. Ha-ras and N-ras regulate MAPK activity by distinct mechanisms *in vivo*. Oncogene, *16:* 1417–1428, 1998.